

Strain-induced incomplete wetting at CuAu(001) surfaces

W. Schweika,¹ H. Reichert,² W. Babik,¹ O. Klein,² and S. Engemann²

¹*Institut für Festkörperforschung, Forschungszentrum Jülich, 52425 Jülich, Germany*

²*Max-Planck-Institut für Metallforschung, D-70569 Stuttgart, Germany*

(Received 17 March 2004; published 12 July 2004)

X-ray reflectivity measurements, modeled on atomic scale by a dynamic approach, reveal a smooth Au top layer and subsequent Cu/Au layering at the (001) surface of CuAu crystals at high temperatures, enforced by a large surface field h_1 . Approaching the first order bulk transition the ordered near surface film grows but does not completely wet its disordered bulk phase as predicted. In contrast to earlier wetting experiments on heterogeneous systems which were dominated by surface roughness, we found strong lattice relaxations and incomplete wetting due to strain.

DOI: 10.1103/PhysRevB.70.041401

PACS number(s): 68.35.Md, 61.10.Kw, 64.60.Cn

Phase transitions in real crystals are affected by the presence of free surfaces¹ and physics near surfaces is characterized by a dimensionality in between two and three dimensions. Missing bonds may reduce the order near a surface, which could lead to surface induced disorder, a wetting phenomenon² that, for example, describes the melting of ice.³ Intuitively, one might not expect the opposite, surface induced order. Experiments and Monte Carlo simulations, however, demonstrated the possibility of stable near surface order in equilibrium with a disordered bulk,⁴ if the surface breaks the symmetry of bulk order.⁵ Two cases can be distinguished: First, in systems with frustrated bulk order, a free surface may reduce frustration and induce *lateral* ordering. In the face-centered-cubic (fcc) structure the (001) lattice planes form a square lattice allowing for unfrustrated ordering, which is more stable than ordering of the 3D fcc structure. The second case is related to the phenomenon of surface segregation. Surface enrichment of one alloy component may induce a *layering* order perpendicular to the surface.⁶ Both ordering mechanisms are competing at CuAu(001) surfaces, although surface induced layering (of AuCuAuCu...) can be expected from the surface segregation tendency of Au found in studies of Cu₃Au. Any possible surface induced layering of AuCu will be accompanied by lattice strain arising at the interface between the phases of different symmetries and lattice parameters, the cubic disordered bulk phase and the surface layer of ordered tetragonal CuAu, see Fig. 1. Surface induced ordering at a crystal surface is a wetting phenomenon by a continuously growing solid surface layer as the transition temperature of bulk ordering is approached, even if the bulk ordering is discontinuous. A major difference to a liquid wetting layer is that the solid cannot relax the accompanying strain at the interface. Gittes and Schick⁷ as well as Speth⁸ have investigated this case theoretically and found that strain imposed by the substrate potential induces a long-range force which, in general, prevents complete wetting. This renders the surface phase transition discontinuous. Gittes and Schick also estimated that the strain field will not be relaxed by the formation of dislocations. In recent wetting experiments it has been found that such strain effects are usually overwhelmed by interfacial roughness changing the scenario back to complete wetting.⁹ In these experiments it

was not possible to prepare the heterogeneous system of molecular hydrogen on a gold substrate with sufficiently smooth surfaces. The homogeneous CuAu system appears to be the ideal candidate to verify the role of strain as theoretically predicted,^{7,8} because it is possible to prepare a microscopically smooth and stable surface above the bulk ordering temperature. This allows us to elucidate the role of strain in wetting phenomena and surface phase transitions, which has attracted much attention by theory.

CuAu is known to exhibit two discontinuous structural phase transformations from the $L1_0$ ground state (CuAu-I) to a long-period superstructure CuAu-II at $T_I=385^\circ\text{C}$ and subsequently into the disordered fcc phase at $T_{II}=410^\circ\text{C}$. For crystals slowly cooled from the disordered phase severe and irreversible deformations are observed from mesoscopic to macroscopic length scales caused by the tetragonality of the ordered CuAu structure. Here we are interested in the equilibrium structure of the near-surface order in the disordered fcc phase. In particular, the concentration profile near the free (001) surface and its temperature dependence will clarify the role of strain and roughness and the asymptotic wetting behavior. Furthermore, it allows to access fundamental thermodynamic parameters, e.g., the effective surface field which determines surface segregation, i.e., the preference of either Au or Cu in the top layer.

Experimentally the concentration profile perpendicular to the surface can be determined by x-ray reflectivity measurements with atomic resolution.¹⁰ We have performed *in situ* x-ray scattering experiments at the HASYLAB beamline W1.1 on single crystalline CuAu(001). The instrument was set up for vertical axis geometry using an x-ray energy of

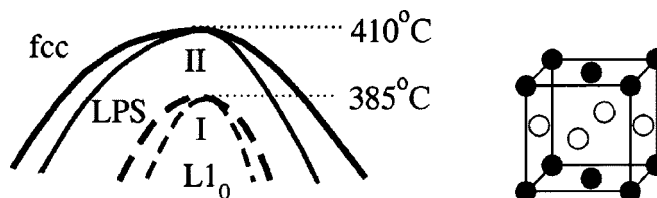


FIG. 1. CuAu phasediagram and $L1_0$ structure.

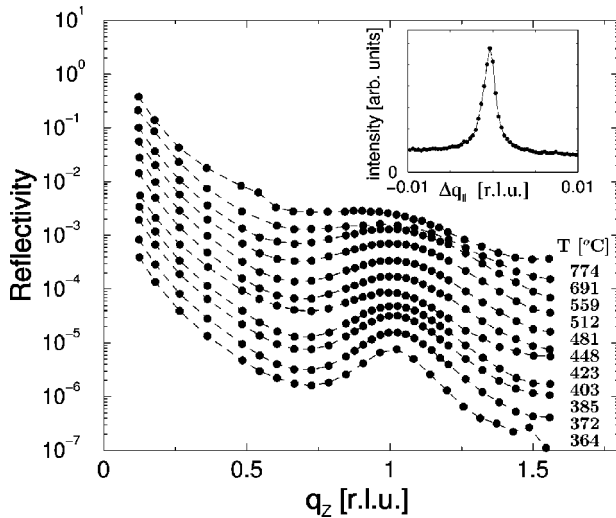


FIG. 2. Temperature dependent reflectivity vs perpendicular momentum transfer in reciprocal lattice units (r.l.u.), as obtained from integrated and background corrected transverse scans. The inset shows a typical transverse scan ($T=774$ °C and $q_z=0.97$ r.l.u.). (Data sets are displaced by factors of 2 with increasing temperature.)

11.0 keV. The crystal was kept in an ultrahigh vacuum chamber equipped with a sputter system. Repeated cycles of sputtering and annealing in the disordered high temperature phase produced a microscopically smooth and clean single crystalline surface. Upon transformation into the ordered phase the surface develops macroscopic roughness due to tetragonal distortions between differently oriented domains. Therefore, reflectivity at small momentum transfer q_z (near the total reflection edge) could not be measured quantitatively. Since the in-plane width varies along the specular path, we performed transverse scans at each q_z in order to retrieve the integrated reflected intensity and to separate background originating from bulk diffuse scattering. A broad peak in the specular intensity, as shown in Fig. 2, is observed near the (001) ordering wave vector, which gives direct information about the excess order perpendicular and near to the (001) surface. Upon decreasing the temperature this peak becomes more pronounced. A straight forward Fourier analysis indicates a growing ordered surface layer on top of a disordered bulk system.

For a quantitative analysis of the reflectivity data either kinematic scattering theory or the more elaborate distorted wave Born approximation could be applied, although neither of the two approaches covers the entire range from total reflection to Bragg scattering correctly. At large q_z values one needs to go beyond the usual continuum approximation including density modulations on an atomic length scale in a dynamic description of the reflected intensity. Therefore, based on the Parratt recursion algorithm,¹¹ we have developed an approach¹² using the realistic electron density distribution on an atomic scale. Starting from tabulated atomic form factors $f(q)$ ¹³ we reconstruct the projected electronic density profile for a single atomic layer including smearing due to species-dependent thermal vibrations by temperature factors $B(T)$:

$$\rho_z(z) = \frac{1}{2\pi} \int_{-\infty}^{\infty} f(q) e^{-B(T)q^2} e^{-iqz} dq. \quad (1)$$

The laterally averaged electron density of the disordered bulk unit cell includes overlapping contributions from neighboring layers z_j :

$$\rho(z) = \sum c_j m_a \rho_z(z - z_j), \quad (2)$$

where $m_a = 2/(2d_o)^2$ denotes the number of atoms per unit area for fcc. A tanh profile is used to describe the oscillating near surface concentration profile (Cu) by the interfacial width ξ and position l_o :

$$c_{oj} = \frac{1}{2} + (-1)^j \left\{ \frac{1}{4} - \frac{1}{4} \tanh[2(z_j - z_s - l_o)/\xi] \right\}. \quad (3)$$

The surface and its roughness is modeled by another independent profile

$$c_j = \frac{1}{2} \left[1 - \operatorname{erf} \left(\frac{z_j - z_s}{\sqrt{2}\sigma} \right) \right] c_{oj}, \quad (4)$$

where z_s and σ define the surface position and roughness. For simplicity and in order to minimize the number of free parameters we assume that the lattice relaxations across the interface, which determine the exact layer positions z_j , follow exactly the concentration profile

$$d_j = \bar{d} + \Delta d \tanh[2(z_j - z_s - l_o)/\xi], \quad (5)$$

where \bar{d} and $2\Delta d$ are the average and the difference of the layer distance in the tetragonal (Ll_o) structure and the disordered fcc bulk. For a numerical calculation of the reflexion/transmission coefficients the electron density profile is sliced into thin layers, which are sufficiently small compared to interatomic spacings. The refinement of the near-surface region can be done very efficiently, since the coefficients for the underlying bulk need to be calculated only once for each perfect scattering angle. We have tested this method and found perfect agreement of our results with the original Darwin theory¹⁴ in the case of semi-infinite monoatomic perfect crystals. Within our approach the measured intensities can be successfully modeled as shown in Fig. 3. One striking result is the extremely small surface roughness, typically less than 0.5 Å for all temperatures. It is measured on a length scale given by the lateral correlation length of typically about 700 Å resulting from the width of transverse scans, see inset Fig. 2. The rigid lattice model cannot account for the observed asymmetry around the (001) superstructure position, which directly relates to lattice relaxations of typically -7% at the surface. This asymmetry is even more pronounced on the truncation rod near the (002) Bragg reflection. Using the model including lattice relaxations we find perfect agreement with the measured data sets for all temperatures. Figure 4 displays the electron density profile (a) which contains the roughness, the concentration and the relaxation profile of the ordered state near the surface. We found surface induced order with the ordered state still existing at temperatures well above the bulk order-disorder transition temperature. The uppermost layer is essentially occupied by pure Au even at temperatures as high as $T=T_1+400$ K. Subsequent deeper

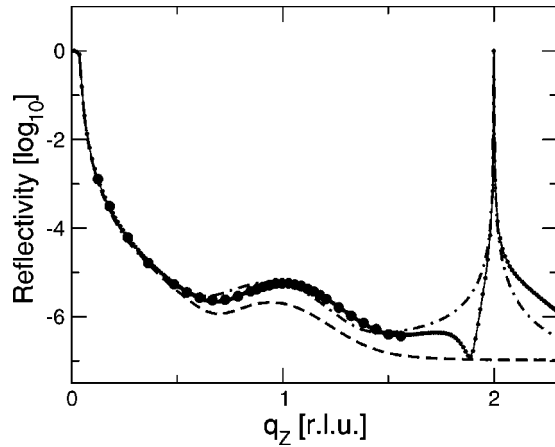


FIG. 3. Calculated reflected intensities at the (001)-surface considering near surface order and lattice relaxation; $T=T_1+96^\circ\text{C}=481^\circ\text{C}$. Filled circles: experimental data; broken line: continuum model; dashed-dotted line: rigid lattice model; solid line: relaxed lattice model.

atomic layers display an oscillating concentration profile and lattice relaxations consistent with the expected tetragonal lattice parameter of the ordered CuAu-I structure. With decreasing temperatures we find an increase of both, position and width of the interface between the ordered surface layer and the disordered bulk. Wetting theory¹ predicts a logarithmic growth of the surface layer thickness, as the temperature

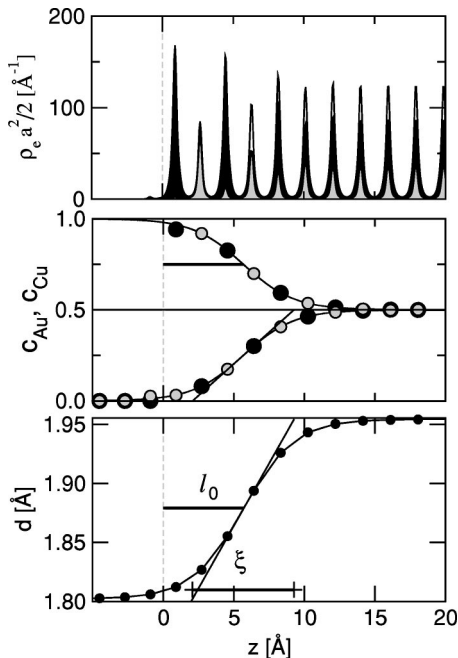


FIG. 4. Near surface order and lattice relaxation (at $T=480.6^\circ\text{C}$, see Fig. 3). Top: electron density depth profile, Au (black), Cu (gray), total (envelope); middle: concentration profiles, c_{Au} (●), c_{Cu} (○); bottom: layer distance. Compositions and layer distances are determined from the electron density profile, and follow a tanh model parametrized by the interfacial position l_0 and interfacial width ξ . Note ρ is small for $z \leq 0$ showing negligible roughness. ($z_s=0$.)

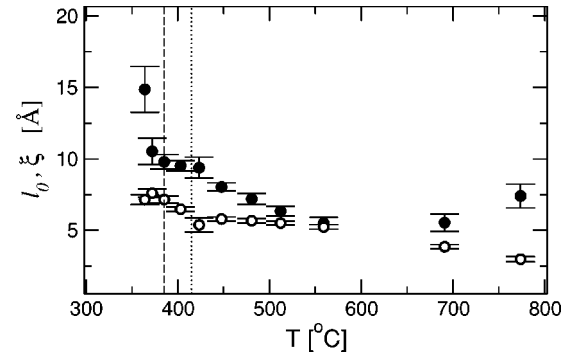


FIG. 5. The temperature dependence of the interface position l_0 (open circles) and width ξ (filled circles). Dashed (dotted) line indicates the bulk ordering temperature $T_1(T_{II})$.

approaches the bulk transition. Even in the supercooled state, however, and close to the bulk transition, the thickness of the near surface ordered layer does not exceed more than a very few atomic layers, see Fig. 5. The ordered surface layer, which is indeed a complete nucleus of the CuAu-I bulk phase, should wet the bulk at the transition near $T_1=385^\circ\text{C}$. Therefore, we conclude that the observed incomplete wetting and possibility of supercooling is a consequence of the induced strain near the surface.

The data at high temperatures can be used to estimate effective surface fields that cause a preference of Au in the uppermost layer. For this purpose we performed Monte Carlo simulations based on an Ising model on a rigid lattice

$$H = - \sum_{ij} J_{ij} s_i s_j - h_i \sum_i s_i, \quad (6)$$

where the sum is taken over bonds between sites i and j . The field h_i is zero in the bulk for equiatomic composition, and is expected to be modified near free surfaces. Two models were considered: (i) the nearest neighbor model, $J_1 < 0$, and (ii) a model including next-nearest neighbors with $J_2 = -J_1/6$, while in both cases the interaction parameters J_{ij} are determined by the bulk ordering temperature T_1 . The simulations yield an estimate for the effective surface field of the first and second layer, $h_{z=1}$ and $h_{z=2}$. A thick slab of 180 layers with 40×40 atoms was embedded at the top and bottom in vacuum ($s_i=0$) applying periodic boundary conditions laterally. The relevant order parameter (OP) for CuAu near the (001) surface is given by $\text{OP} = \frac{1}{2}(1 - 2c_{\text{Au}})(-1)^z$, where z denotes the layer index. Averages of the OP were taken after relaxation to equilibrium. Both models yield similar profiles. An example for $T=691^\circ\text{C}$ is shown in Fig. 6.

Within the nearest neighbor model we estimate an effective surface field $h_{z=1}=170(20)$ meV. The OP profiles are slightly better reproduced within the first few layers using the next-nearest neighbor model with $h_{z=1}=140(15)$ meV and $h_{z=2}=-20(10)$ meV. These estimates are considerably larger than the ordering energy of about $60(10)$ meV. Both models, however, fail to describe in detail the small thickness of the ordered surface layer and the small interfacial width between the ordered surface and disordered bulk phase. This discrepancy can be related to the observed strain effects in-

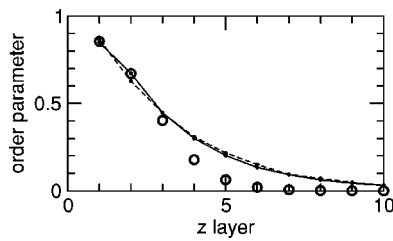


FIG. 6. Order parameter as measured for $T=691$ °C (○) and compared to Monte Carlo simulations on a rigid lattice; (i) dashed line: J_1 model with effective surface field $h_1=170$ meV; (ii) solid line: J_1, J_2 model ($J_2=-J_1/6$) with effective surface fields $h_1=140$ meV and $h_2=-20$ meV. Both, interfacial width ξ and thickness of the ordered layer l are smaller in the measurement than in the simulation, which is attributed to strain effects.

duced by the tetragonally distorted ordered surface layer on the disordered cubic bulk, which are not accounted for in the present rigid lattice simulations. Of course, the discrepancy increases for lower temperatures, where surface induced ordering, a wetting phenomenon, was found in previous Monte Carlo simulations as T approaches the bulk transition temperature.⁶ Monte Carlo simulations including lattice relaxations would be of high interest. Earlier simulation work of this type¹⁵ already showed near-surface order perpendicular to the (001) surface although the wetting behavior was neither discussed nor accessible due to the very limited system size.

Experimentally it is very difficult to determine the magnitude of the surface field h_1 . To our knowledge this has been achieved for only a few systems, e.g., epitaxial FeCo films

grown on MgO substrates which display interface-induced ordering (critical adsorption).¹⁶ In this case the bulk transition is continuous and the order parameter does not couple to the strain field. The pinning of a Co-rich first layer at the interface is mediated by an interface field $h_1=9$ meV that is weak compared to the ordering temperature $k_B T_c=84$ meV. In earlier studies of (001)-surfaces of Cu_3Au ¹⁷ it was also found that the ordering perpendicular to the surface does not diverge at the transition temperature but rather at the spinodal temperature. In the case of Cu_3Au , however, the bulk OP consists of four nonvanishing components. Only the perpendicular component of the order parameter is coupled to the surface,¹⁷ but not the lateral components. For the surface fields we find for the (001) surfaces of Cu_3Au ¹⁸ as well as here for CuAu consistent values of 100–200 meV which are considerably larger than the bulk ordering energy.

In analogy to the melting of ice,³ which cannot be overheated due to the presence of a disordered surface layer acting as a nucleus, the ordered surface layer, which indeed is a complete nucleus of the CuAu-I bulk phase, should wet the bulk at the transition near 410 °C in the absence of lattice strain. From our experiments we find pronounced lattice relaxations perpendicular to the surface although the lateral coherence length remains to be large. The induced lateral strain fields prevent complete wetting as predicted by theory^{7,8} Surface roughness does not change the scenario in CuAu(001) since it is found to be negligible. In future experiments, particularly near the (002) Bragg reflection, we hope to explore the detailed functional form of the relaxation profile.

¹R. Lipowsky, *Ferroelectrics* **73**, 69 (1987).

²S. Dietrich, in *Phase Transitions and Critical Phenomena*, edited by C. Domb and J. Lebowitz (Academic Press, London, 1988), Vol. 12, pp. 1–128.

³A. Lied, H. Dosch, and J. H. Bilgram, *Phys. Rev. Lett.* **72**, 3554 (1994).

⁴W. Schweika, K. Binder, and D. P. Landau, *Phys. Rev. Lett.* **65**, 3321 (1990).

⁵R. Leidl and H. W. Diehl, *Phys. Rev. B* **57**, 1908 (1998).

⁶W. Schweika, D. P. Landau, and K. Binder, *Phys. Rev. B* **53**, 8937 (1996); W. Schweika, D. P. Landau, and K. Binder, in *Stability of Materials*, edited by A. Gonis and P. E. A. Turchi (Plenum Press, New York, 1996), p. 165.

⁷F. T. Gittes and M. Schick, *Phys. Rev. B* **30**, 209 (1984).

⁸W. Speth, *Z. Phys. B: Condens. Matter* **61**, 325 (1985).

⁹A. Esztermann, M. Heni, H. Löwen, J. Klier, M. Sohaili, and P. Leiderer, *Phys. Rev. Lett.* **88**, 055702 (2002).

¹⁰C. Ern, W. Donner, A. Rühm, H. Dosch, B. P. Topoverg, and R. L. Johnson, *Appl. Phys. A: Mater. Sci. Process.* **64**, 383 (1997).

¹¹L. G. Parratt, *Phys. Rev.* **95**, 359 (1954).

¹²W. Babik, Ph.D. thesis, RWTH Aachen, 2002.

¹³*International Tables for Crystallography*, edited by A. J. C. Wilson and E. Prince (Kluwer Academic, Dordrecht, 1999), Vol. C.

¹⁴C. G. Darwin, *Philos. Mag.* **24**, 315 (1914); **24**, 675 (1914).

¹⁵J. Tersoff, *Phys. Rev. B* **42**, 10965 (1990).

¹⁶B. Nickel, F. Schlesener, W. Donner, H. Dosch, and C. Detlefs, *J. Chem. Phys.* **117**, 902 (2002).

¹⁷H. Reichert, P. J. Eng, H. Dosch, and I. K. Robinson, *Phys. Rev. Lett.* **74**, 2006 (1995).

¹⁸W. Schweika and D. P. Landau, in *Computer Simulation Studies in Condensed Matter Physics X*, edited by D. P. Landau, K. K. Mon, and H. B. Schuettler, Springer Proceedings in Physics Vol. 83 (Springer, Berlin, 1998).